Designed Autonomic Motion in Heterogeneous Belousov–Zhabotinsky (BZ)-Gelatin Composites by Synchronicity

*Matthew L. Smith, Connor Slone, Kevin Heitfeld, and Richard A. Vaia**

Critical technologies from medicine to defense are highly dependent on advanced composite materials. Increasingly there is a greater demand for materials with expanded functionality. The state of the art includes a wide range of responsive composites capable of impressive structural feats such as externally triggered shape morphing. Here a different composite concept is presented, one in which a portion of the constituent materials feed off of ambient energy and dynamically couple to convert it to mechanical motion in a cooperative, biomimetic fashion. Using a recently developed self-oscillating gel based on gelatin and the oscillating Belousov–Zhabotinsky (BZ) reaction, a technique is demonstrated for producing continuous patterned heterogeneous BZ hydrogel composites capable of sustained autonomic function. The coupling between two adjacent reactive patches is demonstrated in an autonomic cantilever actuator which converts chemical energy into amplified mechanical motion. The design of heterogeneous BZ gels for motion using a basic finite element model is discussed. This work represents notable progress toward developing internally responsive, bio-inspired composite materials for constructing modular autonomic morphing structures and devices.

1. Introduction

Design and fabrication of composites and meta-materials underpin a rapidly growing number of critical technologies, ranging from transportation and defense, to athletics, radar, communications and medicine. The architecture (structure) determines the novel performance of the composite, producing enhancements over the constituent materials, or even new properties not seen in natural or synthetic bulk materials.[1] Composite concepts however are generally static. Only recently are constituents and associated designs evolving that provide a dynamic character, such as externally triggered morphability (shape change)[2] or tunable susceptibility to stimuli.[2–6] Such bio-inspired material systems, though, still lack a key feature of living systems - autonomic response. In these cases, the dynamic response emerges from the synchronous behavior of internally responsive modular units such as observed in the heart, mammalian musculature, neural processes, and flora tropism. To incorporate such internal responsivity within a composite structure, at least three crucial elements must be available: (1) a material that simultaneously can transduce an ambient energy source into motion, exchange information between nearest neighbor constituents regarding its state, and establish an effective closed-loop feedback control between motion and this state awareness; (2) a processing platform to fabricate monolithic, complex hetero-structures consisting of active and inactive constituents at or below the critical length scales established by communication between, and uniformity of, the active response; and (3) design and modeling tools to a priori predict behavior and optimize architecture for required performance goals.

One path to autonomic behavior has been demonstrated by Yoshida and co-workers, who copolymerized N-isopropylacrylamide with a Ru catalyst complex used in the oscillating Belousov–Zhabotinsky (BZ) reaction[7–12] (see Scott[13] for an approachable treatment of BZ chemistry). These autonomic BZ hydrogels participate *intrinsically* in the oscillating chemical reaction as opposed to responsive hydrogels which react to an arbitrary, programmed, or oscillatory *external* stimulus.[14,15] When the BZ gel is immersed in a solution containing all the BZ reactants except the metal catalyst, periodic, chemically-driven oxidation and reduction of the catalyst occurs only within the hydrogel, affecting the solubility of the network and producing a swell-deswell motion of the gel, i.e., autonomic conversion of chemical to mechanical energy.[16] Recently, several interesting works have placed an emphasis on examining the influence of internal structure on the behavior of homogeneous oscillating gels,[17–19] and on chemical coupling between individual BZ oscillators in close proximity (beads, emulsions, and gel disks).[9,20–26]

The nature of the chemical wave in BZ gels is characterized by a critical length (≈0.8 mm), which is established by the transport of the reactants and products.[27] Samples with one physical dimension greater than this length support a chemical wave propagation across the gel, while those less than the critical length exhibit relatively uniform chemical oscillations; that is, the sample changes fully from the reduced state (typically dark orange) to the oxidized state (light orange to green). The overall strain in long samples (>mm) is thus limited since

Dr. M. L. Smith, C. Slone, Dr. K. Heitfeld, Dr. R. A. Vaia
Air Force Research Laboratory
Materials and Manufacturing Directorate
Wright-Patterson Air Force Base, OH 45433, USA
E-mail: Richard.Vaia@wpafb.af.mil
Dr. K. Heitfeld
Renegade Materials Corp., 3363 South Tech Boulevard
Miamisburg, OH 45342, USA

DOI:10. 1002/adfm.201202769

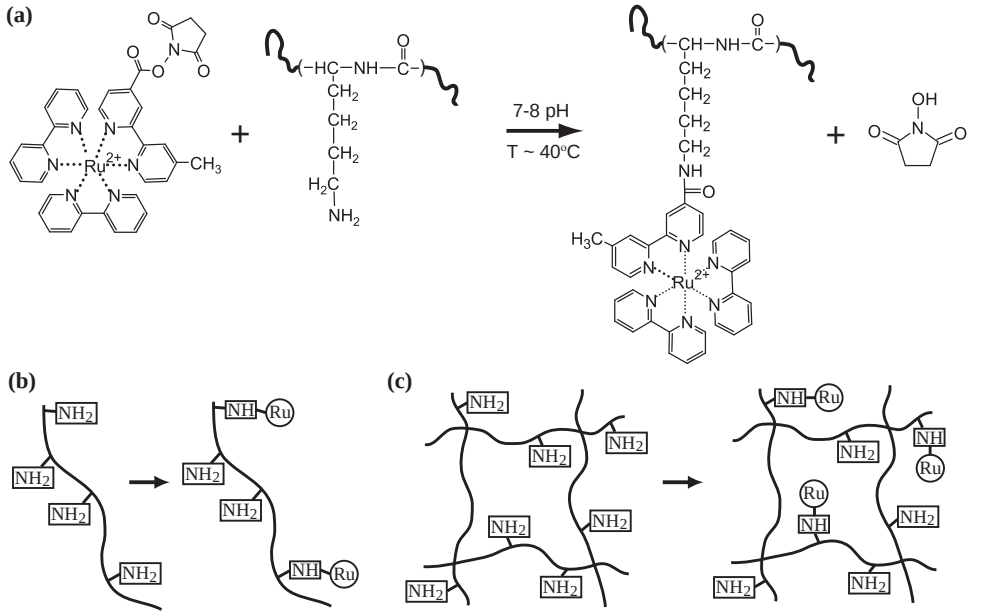

Figure 1. Synthesis of BZ-gelatin. a) Succinimide ester–amine coupling reaction to form an amide linkage between ruthenium succinimide ester bipyridine complexes (Ru(sbpy)) and lysine residues along the gelatin polypeptide chain.[33] This post functionalization chemistry is quite versatile, and is applicable to linking the BZ redox catalyst (b) to gelatin dissolved in solution or (c) to the polymer network after gelation.

offsetting regions of reduced and oxidized catalyst lead to stationary nodes along the long dimension of the gel, and only the residual length of gel beyond the final stationary node affects the amplitude of the periodic length change.[28] On the other hand samples shorter than the chemical wavelength, typically experience uniform, isotropic mechanical swell-deswell oscillations that are in-phase with the chemical waves. The result is a relatively high level of strain. If these sub-mm scale samples could be coupled and combined as modular building blocks, summation of the coordinated strain oscillations could be used to produce amplified and complex motions much like numerous bundles of muscle fiber working in concert.

Yashin and Balazs[29] introduced one possible method for generating cooperative chemomechanical effects between small BZ gel patches, based on patterning the metal catalyst to create a heterogeneous BZ gel. More than individual oscillators in close proximity, a heterogeneous gel incorporates reactive and nonreactive patches that are physically fused,[8,30,31] leading to a continuous composite structure capable of supporting three-dimensional mechanical loads. Through simulation Yashin and Balazs showed that coupling between responsive patches, surrounded and interconnected by non-responsive regions, could be tuned through structural features of the gel such as patch spacing or elastic modulus. This type of control suggests the potential to design a structured, composite autonomic material from modular building blocks to perform cooperative complex functions beyond the capabilities of homogeneous gel systems (cf. Yashin and Balazs[29] and Westbrook and Qi).[31] Unfortunately, the majority of the current suite of self-oscillating gels[7,10,32] are not readily adapted to common soft-matter patterning techniques, such as additive manufacturing and soft-lithography. Thus a material system with facile fabrication and simplified design rules is needed to meet the aforementioned crucial elements to create an autonomic composite with internal responsivity.

Herein, we use the recently developed BZ-gelatin system[8] to fabricate heterogeneous gels, which contain individual oscillators (patches) that exhibit synchronicity and lead to amplified macroscopic motion. Molecularly precise incorporation of the BZ catalyst along the gelatin chain was achieved via post-functionalization of the polypeptide via a conventional succinimide-amine coupling reaction[33] between ruthenium succinimide ester bipyridine complexes (Ru(sbpy)) and lysine residuals. Thermogelling behavior of gelatin[34,35] enables additive manufacturing techniques such as printing using a heated print head and a chilled substrate (4 °C). Various patterns with dimensions greater and less than the critical patch size and spacing can be easily fabricated. In general, the performance of these composite, heterogeneous BZ gels agrees well with linear mechanics models, and thus brings together the crucial elements necessary for designed autonomic behavior from a finite set of modular units and architectures.

2. Results and Discussion

2.1. Heterogeneous BZ Gelatin

To expand the options of self-oscillating materials compatible with a larger range of processing approaches, a self-oscillating gel based on the biomacromolecule, type A gelatin (referred to hereafter as simply gelatin), was recently developed, **Figure 1**.[8] In brief, molecularly precise incorporation of a ruthenium succinimide ester bipyridine complex (Ru(sbpy)) along the polypeptide chain is achieved with a conventional succinimide-amine coupling reaction[33] through lysine residuals (Figure 1a, see

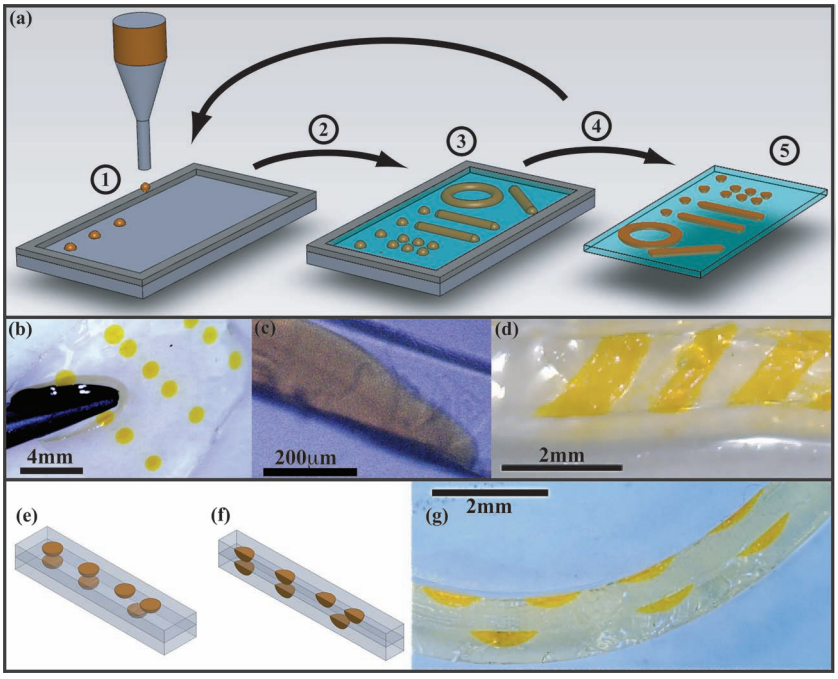

Figure 2. Heterogeneous BZ-Gelatin Composites. a) Patterning process for BZ gelatin. (1) A heated microdispenser (50–55 °C) deposits droplets of melted BZ gelatin on a room temperature slide covered with a fluorinated surface protector. (2) The slide is briefly chilled (4 °C) to solidify the pattern. (3) Additional gelatin (no catalyst) (50–55 °C) is poured over the pattern. (4) A cover slide is placed on top and the assembly is chilled (4 °C). (5) The final patterned sheet is peeled off and placed in a glutaraldehyde solution to chemically crosslink. Alternately, three-dimensional patterns can be printed layer by layer by removing the coverslip after cooling and cycling from (4) back to (1). b) 2D heterogeneous composite BZ-gels with varied spacing, c) cross-section of printed patch perpendicular to film surface, and d) a striped anisotropic layup pattern. e-g) Schematic and cross section of a bent 3D composite BZ-gel with two layers of off-set patches at various spacing (patch diameters ~1 mm, horizontal spacing (edge-to-edge, *w*) ~700 μm and 1.7 mm, vertical patch spacing ~600 μm).

Experimental Section for details). Note that the succinimide-amine coupling reaction is not unique to gelatin. It provides a versatile method for postfunctionalizing any hydrogel (biomacromolecular or synthetic polymer) containing primary amines, such as elastin-like polypeptides[36] or polymers copolymerized with N-(3-Aminopropyl)methacrylamide (APMA); thus providing a means to rapidly expand the available autonomic hydrogels. Catalyst incorporation can be executed in solution yielding Ru-gelatin (gelatin in which a ruthenium catalyst has been anchored) chains (Figure 1b) or after the hydrogel is formed via physical crosslinking or chemical crosslinking with glutaraldehyde (Figure 1c).[37,38] As a result patterning can be achieved either through sequential printing of Ru-gelatin and plain gelatin, or by applying reactive Ru-containing inks to already formed gelatin films (e.g. stamping).

The heterogeneous BZ-gels discussed herein were fabricated by printing heated solutions of Ru-gelatin onto a cold support, followed by further printing of heated solutions of un-functionalized gelatin, **Figure 2**. Gelatin undergoes a reversible melt-gel transition around 30 °C, depending on Bloom strength and gelatin concentration, due to the formation of physical crosslinks through interchain hydrogen bonding.[34,35] This thermogelling behavior makes gelatin amenable to printing techniques using a heated print head or microdispenser. Patch size was controlled by varying pressure and frequency applied to a microdispenser valve. Typical patches have diameters in the interval 800–1000 μm, though patches with diameters down to about 600 μm can be produced with the current system (see Experimental section for details). Patch spacing was controlled by moving the substrate on a biaxial linear stage relative to the dispenser nozzle. After solidifying the pattern by a brief cooling cycle at 4 °C, melted plain gelatin is poured over the top of the Ru-gelatin pattern and the entire assembly cooled. The gelled heterogeneous sheet can be peeled off of the substrate and chemically crosslinked in glutaraldehyde.[37,38] Three dimensional patterns (Figure 2e–g) are produced by sequential printing, that is, after one layer is printed and quickly gelled at 4 °C, a new layer is printed on top. The heat from the hot gelatin causes a thin portion on the surface of the cooled gelatin layer to melt, and so the two layers are fused upon cooling. Using this technique, arbitrarily patterned 2D and 3D sheets can easily be created with varying feature size and inter-patch spacing. This general approach also enables more advanced composite design such as incorporation of material anisotropies, e.g., patterning reactive stripes in addition to patches (Figure 2d).

2.2. Critical Spacing and Synchronicity between Reactive Patches

Figure 3 summarizes the effect on chemical oscillations of spacing (*w*, measured edge-to-edge) between two reactive patches within an inert gelatin matrix. The paired oscillator samples were cut from a larger BZ-gelatin pattern and suspended by a PDMS clamp in a BZ solution containing 0.08 M sodium bromate, 0.02 M malonic acid, and 0.7 M nitric acid (Figure 3a inset). As previously noted by prior studies on homogeneous BZ gels,[8,12] gelatin samples slowly shrank with increased submersion time in the BZ medium (e.g. the diameter, d, of reactive patches decreased from 958 ± 121 μm to 753 ± 131 μm over 6 h). Decreasing patch size can lead to a decrease in period (cf.),[23] though percent strain is not affected. For these solution conditions, heterogeneous gels with single patches exhibit uniform redox oscillations (period, P = 2039 ± 251 s), also consistent with prior reports.[8,12,27] For two-patch samples, stable oscillations commenced almost immediately and the patches always started out in synchrony due to the nearly identical initial conditions. The average periods of these two-patch samples varied between 1100 and 3000 s. The periods showed no clear correlation to inter-patch spacing. In almost all cases the patch located nearest the clamp had a shorter period and acted as a pacemaker. The effect of the clamp and the resultant non-free boundary conditions is likely to reduce diffusion of reaction

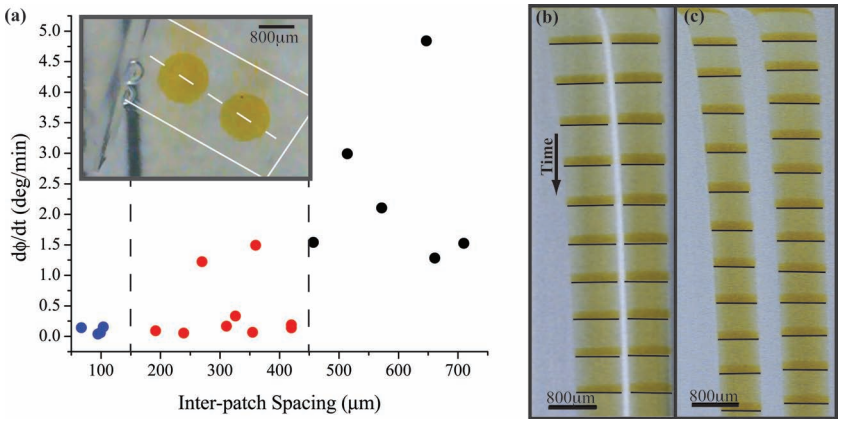

Figure 3. Impact of inter-patch spacing (w) on synchronicity. a) time rate of change of the phase difference ($d\varphi/dt$) between two patches (d ~ 800 μm, average for the first 6 oscillations, to 10 000–15 000 s) within a heterogeneous BZ-gelatin strip (0.08 M sodium bromate, 0.02 M malonic acid, and 0.7 M nitric acid). The inset shows a representative sample (edge highlighted to guide the eye). Each data point reflects a different sample. Color of the data reflects the phase behavior between the pair (blue: ~0°; red: 30°–40° or weak coupling so that phase drift occurs; black: completely uncoupled). Three regions are revealed: strongly coupled in-phase synchronicity; a transition region with weakly coupled synchronicity and entrainment; and decoupled oscillators. b) In-phase synchrony (w ~100 μm, period ~ 1680 s) and c) decoupled oscillations of a pair of BZ gelatin patches (w ~ 390, period of left patch ~ 1580 s, period of right patch ~ 1420 s). The images are formed by lining up a row of pixels (dashed line on inset (a)) across the two patches with time. Black lines were added at the initiation of oxidation in order to guide the eye.

intermediates,[39] such as the autocatalytic agent $HBrO_2$, compared to the patch at the tip of the sample where the oscillations are slower. Alternatively, mechanical force transmitted from the clamp could induce or tune oscillations as predicted by Balazs et al.[40,41] and reported by Chen et al.[9]

The extent of synchronicity, or coupled oscillatory behavior, is summarized with regard to the rate of change of the phase difference between the two patches in Figure 3a. The phase difference ($\varphi = 2\pi(\Delta t_{ox1} - {}_2/p_{low})$) was taken as the difference in time between the initiation of oxidation for the two patches divided by the smallest period (between the two patches) for that oscillation. $d\varphi/dt$ was approximated with a simple divided difference (see the Supporting Information for details of the calculations), and reflects how quickly the phase is shifting between the two patches.

In general three regimes of oscillation were observed. At small inter-patch spacing (w < 150 μm), the patches oscillate in phase (blue: φ ~ 0) and are strongly coupled over the times considered in these experiments (up to 7 h). At slightly larger inter-patch spacing (150 μm < w < 450 μm), some patches still exhibit synchronicity, but with a phase lag (entrainment) where one patch trails the other (red: 30° < φ < 40°). Within this transient region, entrainment remains relatively stable over the times considered in these experiments. However, we also observe that some patches do not entrain and slowly drift out of phase, which is discussed further below. Above a critical spacing (w > 450 μm), the patches never exhibit coupled behavior (black) and behave as independent oscillators with a frequency dictated by their local conditions. Images comparing time-redox behavior for a set of synchronized and a set of uncoupled patches are shown in Figure 3b,c.

According to simulations by Yashin et al.,[42] the characteristic length in a heterogeneous BZ gel is given by $L_o = (D_u T_o)^{1/2}$, where T_o is the characteristic time scale of the problem and D_u is the diffusion coefficient of the dissolved reactant (for a small molecule in water ≈1×10^{-5} cm^2 s^{-1}). In their simulations $L_o \sim 30 - 40\ \mu m$, $T_o \sim 0.6 - 1s$, and they considered spacings from $1L_o$ to $10L_o$.[23,29] The characteristic time scale is given by $T_o = (k_3 HA)^{-1}$, where k_3H is the rate of the autocatalytic process in the BZ reaction, k_3 = 42 M^{-2},[43] H = [H$^+$] is the hydrogen ion concentration, and A = [BrO$^-_3$] is the bromate concentration. From these parameters, the characteristic length under our experimental conditions is ≈30 μm. As such, the regime of strong coupling occurs for patch spacing under about 6 characteristic lengths (~180–200 μm). This estimate agrees well with the model's predictions of strong in-phase coupling for patch spacing within a heterogeneous gel near and above the characteristic length. According to simulations, similar spacing of patches within a non-responsive gel are predicted to exhibit oscillation quenching. Additionally, like the simulations, we observe some cases of stable phase lag at intermediate spacing.[23] The simulations did not consider larger spacing in which patches begin to completely decouple, but given the general agreement with experimental results, decoupling would likely be predicted to occur sometime after $11L_o$ to $13L_o$ (330–390 μm).

The behavior over various patch spacing is also consistent with prior experimental reports of physical assemblies of BZ patches.[20,23,44] For example, Toiya et al. found separations less than ~400 μm were necessary for synchronized chemical coupling of aqueous BZ drops separated by oil within a microfluidic capillary.[44] Fukuda et al.[20] found using cation-exchange beads featuring anchored BZ catalysts, that there was a critical spacing between beads beyond which a pacemaker bead could no longer entrain the other beads in a row. At this critical spacing the degree of entrainment varied drastically from experiment to experiment. They showed through numerical simulation that the degree of entrainment at this critical distance was sensitive to the distribution or small variations in the natural period (the period the oscillator would experience if it were in isolation) of the individual oscillators. That is, there is a critical distance over which the reaction intermediates dissipate to a sufficient degree so that the oscillators cannot communicate strongly enough chemically to entrain one another. Though we are only considering two coupled oscillators, we observed a similar instability in degree of coupling for spacings between 200 and 400 μm. It would seem in this region the strength of the coupling has diminished enough that a sufficiently large discrepancy in the natural period of the individual patches (due perhaps to variations in size, local catalyst concentration, or boundary conditions) can lead to behavior that appears to be decoupled.

2.3. Autonomic Actuators

Control of coupled patch synchrony, period, and mechanical behavior through patterning (modularity), chemistry, and mechanical design presents an excellent opportunity for programming complex motions into autonomous actuators and devices. To demonstrate the potential of this approach we fabricated and examined the operation of one-patch and three-patch bending actuators. These actuators were cut from patterned BZ gelatin sheets, clamped in PDMS, immersed in BZ solution, and videotaped from the side (compare **Figure 4**a). In the case of the actuators, the sides of the samples were cut as close to the edges of the patches as possible to eliminate resistance from excess nonresponsive material. For the BZ solution conditions (0.08 M sodium bromate, 0.02 M malonic acid, and 0.7 M nitric acid), the maximum displacement of an isolated patch (initial diameter ~ 920 μm; diameter at 16 000 s of ~700 μm) and the strain (~1.5%) was in accordance with prior reports.[8]

Both the one-patch and three-patch actuators oscillated mechanically. The one-patch actuators experienced tip displacements of 38 ± 7 μm, about 3.6 times greater than the assumed maximum linear amplitude of an individual patch. The motion amplification is made possible by incorporating the patch into a cantilever configuration. Bending in the cantilever is due to the gradient in strain produced by the asymmetric shape of the patch through the thickness. That is, there is more active material on one surface of the cantilever and it diminishes as the patch rounds off through the thickness (Figure 2c). When three patches are patterned with sufficiently close spacings (i.e., near $10L_o$ or less), they have the potential to couple and oscillate with near in-phase synchrony. Designing actuators with spacings less than $6L_o$ would ensure strong coupling. The result of synchronized operation is coordinated and amplified motion. The three patch actuators we fabricated had total lengths around 4–5 mm and average inter-patch spacings of 297 ± 57 μm, 16 000s after being immersed in BZ solution (for more detailed information on sample dimensions see the Supporting Information). These actuators experienced tip deflections of 162 ± 36 μm, a motion amplification of about 15 times over a single homogeneous BZ patch. As can be seen in Figure 4a the overall deswell response of the BZ patches leads to a cantilever that oscillates about a curved configuration. The x,y displacement of the tip was set to zero for the configuration at 16 000 s and then tracked for four oscillations. The progression of the deflections in the x and y direction with time are shown in Figure 4b. The periodic increase in the deflections correlates to the near-synchronized oxidation of the BZ patches (change from orange to light orange/green).

The preceding results suggest that intelligent patterning of functional BZ units can lead to specialized behavior. Finite element models are useful for predicting optimal ways to combine BZ patch building blocks to achieve desired mechanical functionality. Here we construct a model of the BZ actuators using the finite element software, ABAQUS, and use our experimental results to validate the modeling approach (**Figure 5**). The goal of this model is to capture the magnitudes of the oscillating displacements. To this end we do not include any dynamic processes. Under the BZ solution conditions used

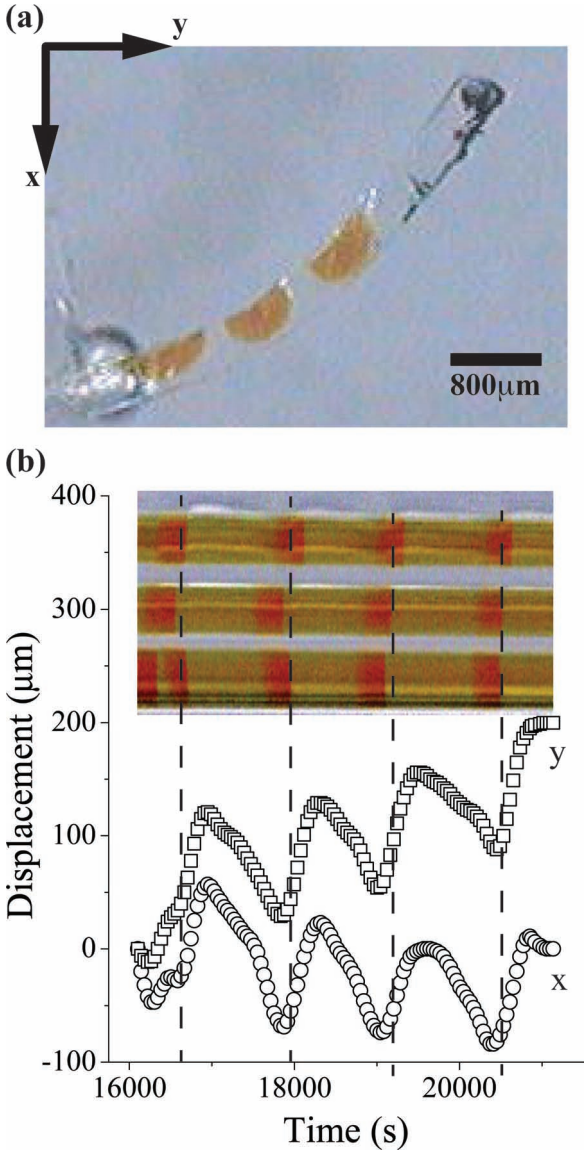

Figure 4. a) Side view of a three patch actuator (at 16 000 s, d ~ 730 μm, w ~ 300 μm) fixed at one end by a PDMS clamp. The tip of the cantilever (upper right) was colored with permanent marker to aid tracking of the tip deflection. b) Periodic tip displacement of a self-oscillating actuator driven by three coupled BZ patches after about 4.5 h in BZ solution (0.08 M sodium bromate, 0.02 M malonic acid, and 0.7 M nitric acid). The image inset shows a row of pixels through the patches that were captured for each video frame and lined up with time. The vertical dashed lines demonstrate the correlation between the oxidation of the patches and the rapid increase in the x and y displacements. The patch closest to the tip is shown on top of the inset. Colors in the inset were enhanced to aid visualization.

in the actuator experiments a homogeneous micron scale BZ gelatin gel will have isotropic strain amplitude of about 1.5%.[8] To model this strain in a controlled fashion we defined the BZ gelatin material to have a negative thermal coefficient of expansion and applied appropriate thermal boundary conditions at the patch surfaces. The nonreactive gelatin in the model was not thermally responsive and the tip deflections were extracted

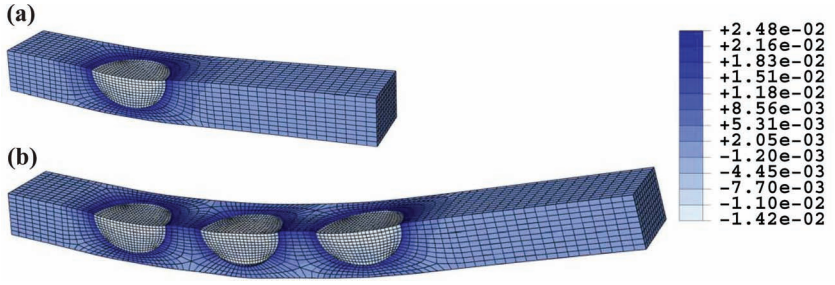

Figure 5. Maximum principal strain profile and deflection of a) one patch and b) three patch composite actuators (d ~ 700 μm, w ~ 280 μm). In the three patch model the patches are assumed to operate in synchrony. The deformations are shown with a 5× amplification to aid visualization; color contours depict principal stain. The range of strain for the one patch model shown above is -1.39×10^{-2} to 2.28×10^{-2}. For further details concerning modeling assumptions, boundary conditions, and dimensions see the Supporting Information.

at steady state. The patches were assumed to be half ellipsoids (cf. Figure 2c). Predicted total tip deflection amplitudes (42 μm and 191 μm for the one patch and three patch actuators respectively) compared well with the measured values (38 ± 7 μm and 162 ± 36 μm). Maximum principal strains of 2.5% occurred just outside the patches and are well within acceptable levels for this material.[37]

For any heterogeneous gel system there will be a critical length (L_d) at which the strains imposed by the patches on the surrounding gel matrix will decay to zero. Regardless of whether the patch spacing is less than or greater than L_d, the strains generated in each patch should lead to additive deformation if chemical coupling can be achieved. In this sense strain coupling between patches may have a limited effect on overall actuator behavior. However, below L_d strain in the surrounding matrix may lead to some mechanical feedback, for example, by affecting diffusion rates of the reactant intermediates via changes in the polymer volume fraction.[41] This mechanical feedback, if significant, is another control avenue for design of heterogeneous gel behavior. For example, beyond simply changing the patch profile through the actuator thickness to affect bending mechanics the patch profile could be optimized to elicit a chemomechanical feedback. Similarly, the elastic modulus and structure of the surrounding inert matrix could be optimized to control the strain field and modulate the strength of the mechanical feedback. Indeed, two architectures with similar 2D layouts could be designed to control the strain field around patches to yield two different behaviors through mechanical or chemical feedback. In light of this discussion, an interesting finding from the finite element simulations is the distance at which the maximum principal strains decay. The strains are zero outside ≈300 μm and less than 0.5% outside 200 μm. Therefore, when the spacing between patches exceeds L_d = 400 μm there is limited or no mechanical coupling between patches. Interestingly, this is also the distance at which we observe loss of synchrony between patches. This finding may be purely coincidental. That is, this may simply be the distance at which the reactant intermediates become too dilute to induce chemical coupling. Further studies are required to determine if there is potentially a significant mechanical feedback element to coupled oscillations in the patterned BZ gels.

3. Conclusions

A key route to augmenting the current suite of functional composite materials is the creation of bio-inspired, autonomic composites. The development of these dynamic, internally responsive materials faces several challenges: discovering materials that effectively transduce ambient energy into different forms of energy and that can dynamically couple with nearby, like entities; designing process and fabrication techniques to generate complex hetero-structures with the necessary length scales and architecture to facilitate a comprehensive range of active responses; and incorporating design and modeling tools to a priori predict performance limits and optimize the system. In this work we have begun to address these challenges. We have developed a self-oscillating hydrogel based on gelatin that combines straightforward synthesis from low-cost, readily available precursors, facile processing into complex shapes, and a straightforward route to patterning self-oscillating regions fused within a non-responsive medium. We observed autonomic chemical and mechanical coupling resulting from internal stimulus and leading to coordinated effort between individual units makes these gels a unique class of materials that mimic many distinctive characteristics of living tissue. In particular, we have established critical design parameters such as patch spacing for robust chemical coupling and critical lengths within which mechanical feedback could occur. Using these results we constructed a simple three patch cantilever actuator that exhibited amplified, coordinated motion due to synchronized swell-deswell of adjacent patches. Further, we discussed a basic modeling strategy for predicting and optimizing mechanical motions stemming from coordinated oscillations.

Despite the advancements presented here many challenges, both with regard to design and fabrication of composite BZ gels as well as the physical properties of the gel and solution, remain before practical applications can be realized. Although the BZ-gelatin and post-functionalization synthesis routes discussed provide avenues toward tougher, more robust material platforms, the conditions of BZ solution are caustic and limiting for many applications. Better control of feature size along with a streamlining of gel fabrication is necessary for higher throughput and accuracy in experimentation and for technological viability. Current computational models for self-oscillating gels need to be improved including quantification of unknown model parameters and more accurate prediction of coupling dynamics including accurate time scales and unstable dynamics in the transition zone. Experimental and computational studies need to be performed to establish whether mechanical feedback mechanisms transmitted through the inert matrix are involved in the observed synchrony between reactive patches and how this can be used as a control parameter to optimize material behavior. Finally, new architectures beyond simple dots need to be established, e.g., rational incorporation of mechanical instabilities for reversible fast and large, global motions. Overall however, this work demonstrates that all the elements of an effective autonomous composite can be combined in one

material system. The potential to rapidly manufacture complex architectures with autonomous behavior demonstrates a substantial advancement toward autonomic devices for biomedical and defense technologies, such as sensors, energy conversion, microfluidics, and soft robotics.

4. Experimental Section

BZ Gelatin Synthesis: All water was ultra-pure, double distilled and double deionized, and prepared in house. All chemicals were used as received. A gelatin stock solution was prepared by dissolving 2 g of type-A gelatin (Sigma-Aldrich) in 20 mL of pH 7.4 sodium phosphate buffer. The stock solution (≈pH 7.1) was allowed to gel and stored at 4 °C for later use. To make BZ gelatin, Bis (2,2′-bipyridine) 4′-methyl 4-carboxybipyridine ruthenium N-succinimidyl ester bis(hexafluorophosphate) (Ru(sbpy), Sigma-Aldrich) and the gelatin stock were combined in a ratio of approximately 1.6:98.4 by weight (typically 4.1 mg of Ru(sbpy) and 250 mg of gelatin stock). The gelatin stock was first melted in a small vial at 40 °C. Ru(sbpy) was added incrementally every 15 min in roughly equal quantities (7–8 additions) while slowly stirring (80–100 rpm). After the first three additions 10 µL of N,N-Dimethylformamide (DMF, Sigma-Aldrich) were added along with each Ru(sbpy) addition to aid dissolution. In addition, it was occasionally helpful to raise the temperature briefly to 50 °C to dissolve the Ru(sbpy) into solution.

Fabrication of BZ Gelatin Composites: The BZ gelatin solution was placed in a heated reservoir for a microdispenser system (The Lee Company, 062 MINSTAC, VHS M/2 valve). Glass slides with 400 µm spacers around the perimeter and lined with a fluorinated surface protector (Bytac) were placed under the dispenser valve and their position dictated by a motorized stage controlled by a custom code written in Visual Basic. The spacers were made by layering strips of Bytac. To eject droplets of BZ gelatin, the dispenser is pressurized and the valve opens and closes with a specified frequency. For this work the reservoir and dispenser valve were maintained at approximately 50 °C using heating tape, a thermocouple, and a temperature controller. Typical pressures and frequencies used were ≈25 psi and 150 Hz. Some adjustment of these settings was required from batch to batch and often within a patterning procedure as the viscosity of the BZ gelatin mixture showed some variability. Patterning proceeded as depicted in Figure 1: ① After the BZ gelatin was melted, the heated microdispenser (50–55 °C) deposited droplets of melted BZ gelatin on the room temperature, Bytac covered slide. ② The slide was covered to prevent evaporation of water out of the gel and briefly chilled (4 °C) for 5–10 min to solidify the pattern. ③ Additional gelatin (no catalyst, gelatin stock produced with DI water rather than buffer, pH < 7, and termperature ≈45 °C) was poured over the pattern. ④ Immediately, a cover slide (also covered in Bytac) was placed on top and the assembly was chilled (4 °C) for at least 30 min. ⑤ The final patterned and cooled sheet was peeled off and quickly placed in 10 mL of 5 mM, room temperature, glutaraldehyde (GA, Sigma-Aldrich) solution to chemically crosslink for 24 h. The three dimentsional patterns were produced by printing on top of completed patterned sheets. Instead of using a flat cover slip to cover the layered 3D gel a coverslip with spacers was used to allow for the added height. Gelatin patterned with stripes were created by laying up thin strips of BZ gelatin and then adding plain gelatin (no catalyst, stock produced with DI water, ≈45 °C) over the top and then chilling and crosslinking as above. Using a more sophisticated printer these lined patterns could also be printed. After crosslinking, the patterned gels were rinsed in ultrapure water (fresh water every 24 h for three days), and were stored in DI water at 4 °C. Samples retained their integrity for a minimum of 10 weeks. At higher temperatures or longer storage times the samples can be susceptible to degradation by mold or other biological agents.

Characterization: BZ solution without the metal catalyst was prepared by dissolving sodium bromate (0.08 M) and malonic acid (0.02 M) in nitric acid (0.7 M) (all from Sigma-Aldrich). For characterization of chemical wave periods and synchrony, the patterned BZ gelatin films were cut into strips containing 1 or 2 patches. Generally, we attempted to cut samples so that the edges were about one patch radius from the patch edge (see Figure 2a). The samples were fixed at one end using a slit piece of PDMS for a clamp and then immersed in the BZ solution. The nature of the PDMS clamp ensured the sample was suspended off the bottom of the petri dish holding the BZ solution. Video of the top of the samples was recorded using a Sony SSC-C370 CCD video camera under ambient light conditions at room temperature (ca. 20 °C) for 5–7 h. It is well known that the grayscale intensity can be used to indicate the level of oxidized catalyst in the BZ reaction.[45,46] Therefore, the video was converted to grayscale, and the average grayscale intensity for a small fixed area in each patch on the gel was measured for the duration of the recorded video using the image processing toolbox in Matlab. The chemical wave period and phase were determined by measuring the times at which the rapid periodic oxidation initiated. To characterize tip displacements in 1 or 3 patch actuators a similar method was followed, only samples were cut so that the edges were as close to the sides of the patches as possible and the video was shot from the side of the sample. Displacement measurements and the figures in which rows of pixels are captured and placed together (reslice) with time (Figure 3b, Figure 4b) were generated in ImageJ. The tip displacement measurements were adjusted to account for variations in the distance from the last patch to the cantilever tip in individual samples. Actuator experiments were repeated at least two additional times for each sample type.

Supporting Information

Supporting Information is available from the Wiley Online Library or from the author.

Acknowledgements

This research was performed while M.L.S. held a National Research Council Associateship Award at the Air Force Research Laboratory. The authors gratefully acknowledge partial funding from the Air Force Office of Scientific Research, Lawrence Brott for use of and assistance with the microdispenser printer, and discussions with A. Balazs, Y. Yashin, O. Kuksenok.

Received: September 24, 2012
Revised: November 12, 2012
Published online: January 16, 2013

[1] Y. Liu, X. Zhang, *Chem. Soc. Rev.* **2011**, *40*, 2494.
[2] Q. Meng, J. Hu, *Compos., Part A* **2009**, *40*, 1661.
[3] K. M. Lee, H. Koerner, R. A. Vaia, T. J. Bunning, T. L. White, *Soft Matter* **2011**, *7*, 4318.
[4] X.-J. Han, Z.-Q. Dong, M.-M. Fan, Y. Liu, J.-H. li, Y.-F. Wang, Q.-J. Yuan, B.-J. Li, S. Zhang, *Macromol. Rapid Commun.* **2012**, *33*, 1055.
[5] J. Leng, X. Lan, Y. Liu, S. Du, *Prog. Mater. Sci.* **2011**, *56*, 1077.
[6] Z. He, N. Satarkar, T. Xie, Y.-T. Cheng, J. Z. Hilt, *Adv. Mater.* **2011**, *23*, 3192.
[7] R. Yoshida, *Adv. Mater.* **2010**, *22*, 3463.
[8] M. Smith, K. Heitfeld, C. Slone, R. A. Vaia, *Chem. Mater.* **2012**, *24*, 3074.
[9] I. C. Chen, O. Kuksenok, V. V. Yashin, A. C. Balazs, K. J. Van Vliet, *Adv. Funct. Mater.* **2012**, *22*, 2535.
[10] I. Konotop, I. Nasimova, N. Rambidi, A. Khokhlov, *Polym. Sci., Ser. B* **2009**, *51*, 383.
[11] R. Yoshida, T. Takahashi, T. Yamaguchi, H. Ichijo, *J. Am. Chem. Soc.* **1996**, *118*, 5134.

[12] R. Yoshida, M. Tanaka, S. Onodera, T. Yamaguchi, E. Kokufuta, *J. Phys. Chem. A* **2000**, *104*, 7549.
[13] S. K. Scott, *Oscillations, Waves, and Chaos in Chemical Kinetics*, Oxford University Press, New York **1994**.
[14] T. Tanaka, *Phase-Transitions of Gels,* Vol. *480,* (Eds: R. S. Harland, R. K. Prud'homme) American Chemical Society, Washington **1992**.
[15] P. D. Topham, J. R. Howse, C. J. Crook, S. P. Armes, R. A. L. Jones, A. J. Ryan, *Macromolecules* **2007**, *40*, 4393.
[16] A. N. Zaikin, A. M. Zhabotinsky, *Nature* **1970**, *225*, 535.
[17] Y. Zhang, N. Li, J. Delgado, Y. Gao, Y. Kuang, S. Fraden, I. R. Epstein, B. Xu, *Langmuir* **2012**, *28*, 3063.
[18] Y. Zhang, N. Li, J. Delgado, N. Zhou, R. Yoshida, S. Fraden, I. R. Epstein, B. Xu, *Soft Matter* **2012**, *8*, 3056.
[19] O. Kuksenok, V. V. Yashin, M. Kinoshita, T. Sakai, R. Yoshida, A. C. Balazs, *J. Mater. Chem.* **2011**, *21*, 8360.
[20] H. Fukuda, N. Tamari, H. Morimura, S. Kai, *J. Phys. Chem. A* **2005**, *109*, 11250.
[21] J. Delgado, N. Li, M. Leda, H. O. Gonzalez-Ochoa, S. Fraden, I. R. Epstein, *Soft Matter* **2011**, *7*, 3155.
[22] A. F. Taylor, M. R. Tinsley, F. Wang, Z. Huang, K. Showalter, *Science* **2009**, *323*, 614.
[23] V. V. Yashin, S. Suzuki, R. Yoshida, A. C. Balazs, *J. Mater. Chem.* **2012**, *22*, 13625.
[24] I. R. Epstein, V. K. Vanag, A. C. Balazs, O. Kuksenok, P. Dayal, A. Bhattacharya, *Acc. Chem. Res.* **2011**.
[25] P. Dayal, O. Kuksenok, A. Bhattacharya, A. C. Balazs, *J. Mater. Chem.* **2012**, *22*, 241.
[26] D. Suzuki, T. Sakai, R. Yoshida, *Angew. Chem. Int. Ed.* **2008**, *47*, 917.
[27] R. Aihara, K. Yoshikawa, *J. Phys. Chem. A* **2001**, *105*, 8445.
[28] R. Yoshida, E. Kokufuta, T. Yamaguchi, *Chaos* **1999**, *9*, 260.
[29] V. V. Yashin, A. C. Balazs, *Phys. Rev. E* **2008**, *77*, 046210.
[30] M. L. Smith, K. Heitfeld, M. Tchoul, R. A. Vaia, "Chemical wave characterization of self-oscillating gelatin and polyacrylamide gels," *in Bioinspiration, Biomimetics, and Bioreplication*, Proc. SPIE, *7975* doi:10.1117/12.880939.
[31] K. K. Westbrook, H. J. Qi, *J. Intell. Mater. Syst. Struct.* **2008**, *19*, 597.
[32] S. Nakamaru, S. Maeda, Y. Hara, S. Hashimoto, *J. Phys. Chem. B* **2009**, *113*, 4609.
[33] G. T. Hermanson, *Bioconjugate Techniques*, Elsevier, Amsterdam **2008**.
[34] N. G. Parker, M. J. W. Povey, *Food Hydrocolloids* **2012**, *26*, 99.
[35] M. C. Gómez-Guillén, B. Giménez, M. E. López-Caballero, M. P. Montero, *Food Hydrocolloids* **2011**, *25*, 1813.
[36] S. R. MacEwan, A. Chilkoti, *Pept. Sci.* **2010**, *94*, 60.
[37] A. Bigi, G. Cojazzi, S. Panzavolta, K. Rubini, N. Roveri, *Biomaterials* **2001**, *22*, 763.
[38] Y. Wine, N. Cohen-Hadar, A. Freeman, F. Frolow, *Biotechnol. Bioeng.* **2007**, *98*, 711.
[39] B. Amsden, *Macromolecules* **1998**, *31*, 8382.
[40] O. Kuksenok, V. V. Yashin, A. C. Balazs, *Soft Matter* **2009**, *5*, 1835.
[41] V. V. Yashin, K. J. Van Vliet, A. C. Balazs, *Phys. Rev. E* **2009**, *79*, 046214.
[42] V. V. Yashin, A. C. Balazs, *J. Chem. Phys.* **2007**, *126*, 124707.
[43] T. Amemiya, T. Ohmori, T. Yamaguchi, *J. Phys. Chem. A* **2000**, *104*, 336.
[44] M. Toiya, V. K. Vanag, I. R. Epstein, *Angew. Chem. Int. Ed.* **2008**, *47*, 7753.
[45] S. C. Müller, T. Plesser, B. Hess, *Physica D* **1987**, *24*, 71.
[46] R. Yoshida, S. Onodera, T. Yamaguchi, E. Kokufuta, *J. Phys. Chem. A* **1999**, *103*, 8573.